Temperature-Driven Self-Doping in Magnetite

Hebatalla Elnaggar, Silvester Graas, Sara Lafuerza, Blanka Detlefs, Wojciech Tabiś, Mateusz A Gala, Ahmed Ismail, Ad van der Eerden, Marcin Sikora, Jurgen M Honig, et al.

▶ **To cite this version:**

Hebatalla Elnaggar, Silvester Graas, Sara Lafuerza, Blanka Detlefs, Wojciech Tabiś, et al.. Temperature-Driven Self-Doping in Magnetite. Physical Review Letters, 2021, 127 (18), pp.186402. ⟨10.1103/PhysRevLett.127.186402⟩. ⟨hal-03844658⟩

HAL Id: hal-03844658

https://hal.science/hal-03844658v1

Submitted on 8 Nov 2022

HAL is a multi-disciplinary open access archive for the deposit and dissemination of scientific research documents, whether they are published or not. The documents may come from teaching and research institutions in France or abroad, or from public or private research centers.

L'archive ouverte pluridisciplinaire **HAL**, est destinée au dépôt et à la diffusion de documents scientifiques de niveau recherche, publiés ou non, émanant des établissements d'enseignement et de recherche français ou étrangers, des laboratoires publics ou privés.

HAL Authorization

Temperature driven self-doping in magnetite

Hebatalla Elnaggar,[1,2,*] Silvester Graas,[1] Sara Lafuerza,[3] Blanka Detlefs,[3] Wojciech Tabiś,[4,5] Mateusz A. Gala,[4] Ahmed Ismail,[1] Ad van der Eerden,[1] Marcin Sikora,[6] Jurgen M. Honig,[7] P. Glatzel,[3] and Frank de Groot[1,†]

[1]*Debye Institute for Nanomaterials Science, 3584 CG Utrecht, The Netherlands*

[2]*Sorbonne Université, CNRS UMR 7590, Institut de Minéralogie, de Physique des Matériaux et de Cosmochimi, 4 Place Jussieu, 75005 Paris, France*

[3]*European Synchrotron Radiation Facility, CS40220, F-38043 Grenoble Cedex 9, France.*

[4]*Faculty of Physics and Applied Computer Science, AGH University of Science and Technology, Mickiewicza 30, 30-059 Krakow, Poland.*

[5]*Institute of Solid State Physics, TU Wien, A-1040, Vienna, Austria.*

[6]*Academic Centre for Materials and Nanotechnology, AGH University of Science and Technology, Mickiewicza 30, 30-059 Krakow, Poland.*

[7]*Department of Chemistry, Purdue University, West Lafayette, Indiana 47907-2084, USA.*

Abstract

Magnetite is one of the most fascinating materials exhibiting the enigmatic first-order Verwey transition which is conventionally manipulated through chemical doping. Here we show that heating magnetite results in a spontaneous charge reordering and consequently a hole self-doping effect at the octahedral sublattice. Core level x-ray spectroscopy measurements combined with theory uncovers that there are three regimes of self-doping that map the temperature dependence of the electrical conductivity and magnetism up to the Curie temperature. Our results provide an elegant analogy between the effect of chemical doping and temperature-driven self-doping on trimerons in magnetite.

Magnetite (Fe_3O_4) is one of the most abundant iron bearing minerals on earth and finds many applications in areas such as palaeomagnetism [1–3], medicine [4], data recording [5] and ultrafast magnetic sensors [6, 7] among others [8].It is the first example for an oxide to show a metal to insulator transition (the Verwey transition at $T_V \approx 123\,K$ [9]). Fe_3O_4 has a cubic inverse spinel structure above T_V with Fe^{2+} occupying octahedral interstatial sites (B-sites) while Fe^{3+} are equally distributed over the octahedral and teterahedral interstatial sites(A-sites) [10]. The cubic structure of Fe_3O_4 distorts to a monoclinic superstructure (Cc space group symmetry) below T_V forming a complex network of linear orbital molecules composed of three Fe B-site units called trimerons [11].

Short-range structural fluctuations linked to the presence of trimerons were reported to exist up to the Curie temperature using interatomic pair distribution function derived from total x-ray scattering data [12], diffuse scattering [13] and resonant inelastic x-ray scattering [14, 15]. These structural fluctuations emerge from the magnetic ordering and are regarded as the primary electronic instability at the origin of the Verwey transition [12, 16]. Unveiling the mechanism behind the collapse of structural correlations in magnetite and the temperature evolution of trimerons would significantly shape our understanding of the Verwey transition.

We performed Fe K_{α_1} high-energy resolved fluorescence-detected x-ray absorption spectroscopy (HERFD-XAS) measurements at ID26 of the European Synchrotron Radiation Facility [17, 18] (Fig.1(a)) as a function of temperature on a stoichiometric single crystal of Fe_3O_4 (Fig. S8 and S9). HERFD-XAS spectra are measured with a fluorescence detector such that the life time broadening of the $1s$ core hole no longer appears in the spectra [19]. Two regions of the spectrum can be identified:(i) the K pre-edge from 7110 eV to 7120 eV, and (ii) the K main-edge from 7120 eV to 7200 eV shown in Fig. S1. The spectral shape and the intensity of the K pre-edge is sensitive to the local site symmetry while the K main-edge energy position is indicative of the average oxidation state of all absorbing ions [20, 21]. We found that the main edge position remains almost constant indicating that the overall oxidation state is preserved (Fig. S5 and S6), however spectral changes are observed in the K pre-edge region in Fig.1(a). The intensity of the K pre-edge is redistributed at higher temperatures in a manner which cannot be accounted for by a Boltzmann population of excited states or phonons (see supplementary). The intensity of the K pre-edge peak asymmetrically broadens towards lower energies suggesting a reordering of the Fe charges.

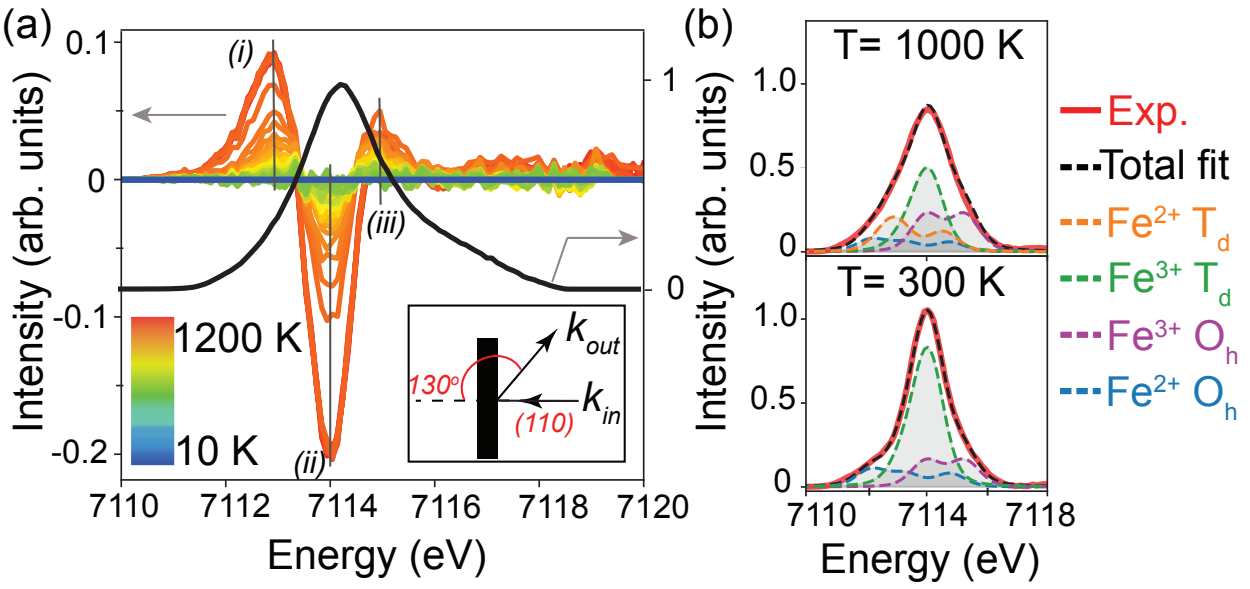

FIG. 1. Fe K_{α_1} HERFD-XAS in Fe_3O_4 measured from 10 K to 1200 K. (a) An exemplary Fe K pre-edge measurement at $T = 300$ K and the difference signal of the Fe K pre-edge as a function of temperature referred to the lowest measurement at $T = 10$ K. A sketch of the scattering geometry is shown in the inset. (b) The K pre-edge at $T = 300$ K (bottom) and $T = 1000$ K (top) together with theoretical simulations using a ligand field multiplet model (dashed lines) illustrating the contributions of the various Fe sites to the spectrum. T_d and O_h stand for tetrahedral and octahedral sites respectively.

The K pre-edge is a powerful tool to study the charge redistribution among octahedral and tetrahedral sites as it acts as a "magnifying glass" (with a magnification of about 4× as determined from our previous work using K pre-edge XMCD and XMLD [22]) directed towards tetrahedral sites. The K pre-edge is formally attributed to quadrupole transitions from the $1s$ electrons to the empty $3d$ orbitals (in many-body language, quadrupole transitions between the $1s^2 3d^n \rightarrow 1s^1 3d^{n+1}$ configurations). This is indeed the case for octahedral sites giving rise to a weak K pre-edge intensity. The situation is different for tetrahedral sites because they lack centrosymmetry which allows for $3d$-$4p$ orbital mixing [23]. Consequently, the K pre-edge gains intensity from both electric quadrupole and partially allowed dipole transitions leading to an intense K pre-edge. Any change in the tetrahedral sites is enhanced which allows us to effectively quantify charge reordering between the two sites.

The contributions of the three Fe sites to the K pre-edge of Fe_3O_4 at room temperature

are shown in Fig.1(b) using ligand field multiplet calculations [24–27]. The main intensity of the K pre-edge arises from the tetrahedral sites (plotted in green) despite the fact that only $\frac{1}{3}$ of the Fe sites reside in tetrahedral sites while $\frac{2}{3}$ reside in octahedral sites (plotted in purple and blue). Theoretical simulations show that the intensity redistribution of the K pre-edge of Fe_3O_4 at 1000 K is a result of a charge redistribution between octahedral and tetrahedral sites. The contribution of Fe^{3+} in tetrahedral sites (green) decreases and a new contribution related to the presence of Fe^{2+} in tetrahedral sites (orange) rises. We note that the proposition that Fe reorders in Fe_3O_4 at higher temperatures was previously suggested based on thermopower measurements [28], neutron powder diffraction [29] and Mössbauer spectroscopy [30, 31]. A concrete analysis of the redistribution has been so far lacking because deducing the cation occupation from macroscopic thermopower measurements depends on the details of the model used while extensive neutron scattering measurements combined with bond valence sum estimates are missing. Although Mössbauer spectroscopy provides this information, there are some inconsistencies in quantification between studies possibly related to the qualities of crystals used.

We quantified the site occupation of Fe^{3+} and Fe^{2+} ions in octahedral and tetrahedral interstitial sites using ligand field multiplet calculations as a function of temperature (see Fig.2 and Fig. S4 showing an exemplary fit). A clear trend is observed: Fe^{2+} progressively decreases in octahedral and increases in tetrahedral sites as the temperature is increased. A counter effect also takes place where Fe^{3+} decreases in tetrahedral sites and increases in octahedral interstitial sites. This redistribution can be parametrised using two variables, α and β, as described by Eqn. 1.

$$\alpha Fe^{2+}_{O_h} + \beta Fe^{3+}_{T_d} + (8-\alpha) Fe^{2+}_{T_d} + (16-\beta) Fe^{3+}_{O_h} \tag{1}$$

The parameters $\alpha = \beta = 8$ describe an inverse spinel structure. On the other extreme, $\alpha = \beta = 0$ describe a normal spinel structure. Intermediate structures are also possible with $\alpha \neq \beta$. The total number of Fe and charge stays conserved, however, the total number of Fe in the octahedral and tetrahedral interstitial sites changes for $\alpha \neq \beta$. The evolution of the α and β parameters as a function of temperature is shown in Fig. 3(a). We can identify three main regimes based on the behaviour of the α and β parameters as a function of temperature:

1. T $\leq$ 330 K: The local charge distribution is preserved over this temperature range and

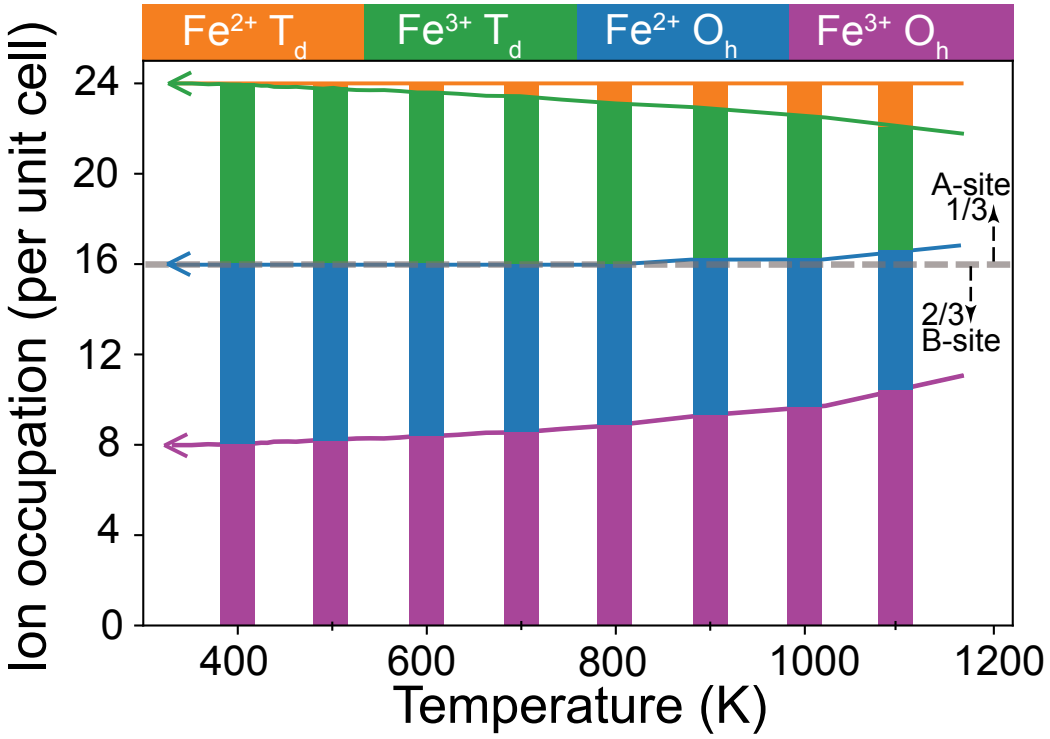

FIG. 2. Occupation of Fe^{3+} and Fe^{2+} ions in octahedral (O_h, plotted in purple and blue) and in tetrahedral (T_d, plotted in green and orange) sites per unit cell of Fe_3O_4 shown for the temperatures between 300 K-1200 K where we observe charge redistribution. The vertical bars are shown to guide the eye. Note that the total Fe charge remains constant (see text).

resembles that of the low temperature phase.

2. 330 K $\leq$ T $\leq$ 840 K: The charge redistributes between the octahedral and tetrahedral sites in this temperature range. This regime is identified by an initial linear subrange to 500 K followed by a significant exponential temperature dependence with $\alpha = \beta$. A full charge is exchanged between the octahedral and tetrahedral sublattices at T = 840 K where the unit cell becomes: $[Fe_1^{2+}, Fe_7^{3+}]_{T_d}[Fe_7^{2+}, Fe_9^{3+}]_{O_h}O_{32}$.

3. T $\geq$ 840 K: The onset of the last regime is identified by a deviation from the equality between α and β. This implies that cations are exchanged between the two sublattices where Frenkel-type point defects are formed [32] and the occupation of the interstitial B sites increases ($\alpha > \beta$). At the highest temperature of our measurement, we find that the unit cell becomes: $[Fe_2^{2+}, Fe_5^{3+}]_{T_d}[Fe_6^{2+}, Fe_{11}^{3+}]_{O_h}O_{32}$.

We performed principle component analysis (PCA) to mathematically confirm the need

of two independent parameters (linear combinations of α and β) to explain the variation in our data across the full temperature range [33]. Fig. S12 shows the PCA results where two principle components are required to explain the experimental data and carry accumulatively 99.95% of the variance. To our knowledge, this is the first work revealing the existence of this intermediate charge distribution intertwined with point defects in stoichiometric Fe_3O_4. These defects behave as an ideal solute according to the extended work of Diekmann and coworkers on oxygen activity in Fe_3O_4 [32, 34–38]. This is also inline with reported kinetics of diffusion in doped ferrites that show that interlattice diffusion processes become relevant for T$\sim$ 500 °C [39]. Results from neutron and x-ray diffraction report an anomalous expansion in the dimensions of the tetrahedral polyhedrons above the T_C, while the expansion of the octahedral polyhedrons remains monotonous [29, 40]. A possible explanation could be due to the significant increase of $[\frac{Fe^{2+}}{Fe^{3+}}]_A$ (with $\alpha > \beta$) and taking into account the larger radius of Fe^{2+} with respect to Fe^{3+} cations (see Fig. S11). However, this remains to be validated with rigorous refinement of diffraction experiments above T_C.

The three charge ordering regimes match the evolution of key physical properties of Fe_3O_4 exquisitely well. For example, the temperature dependence of the electrical conductivity of Fe_3O_4 maps on to the three regimes as can be seen in Fig. 3(b). The electrical conductivity increases from T_V to about 330 K ($\alpha = \beta = 8$) exhibiting a semi-conductor-like behaviour. This is then followed by regime II where the charge ordering parameters begin to decrease and is marked by a decrease in the conductivity with temperature as typical for metal-like behaviour. A saddle point is seen as a minimum in the derivative signal in Fig. S10 corresponding to T= 500 K which corresponds to the end of a linear subrange of regime II. Finally, a modest rise of the conductivity with temperature is observed marking the onset of the third regime at temperatures above 840 K.

A useful way to think about the temperature dependent evolution of the $[\frac{Fe^{2+}}{Fe^{3+}}]_B$ is in terms of B-site hole self-doping in analogy to the widely studied chemical doping of Fe_3O_4 [41, 42]. This is because one expects to find analogies at critical doping levels given that the fundamental building block of the low temperature charge-ordered structure, the three-site linear magnetic polaron referred to as trimeron, persists beyond T_V and up to T_C as seen in Fig. S10(c) [12]. It is possible to evidence the multi-site trimerons in Fe_3O_4 using XAS through the accompanying local Jahn-Teller distortion at the central Fe^{2+} ion, however, our data cannot provide information about the lattice distribution of trimerons.

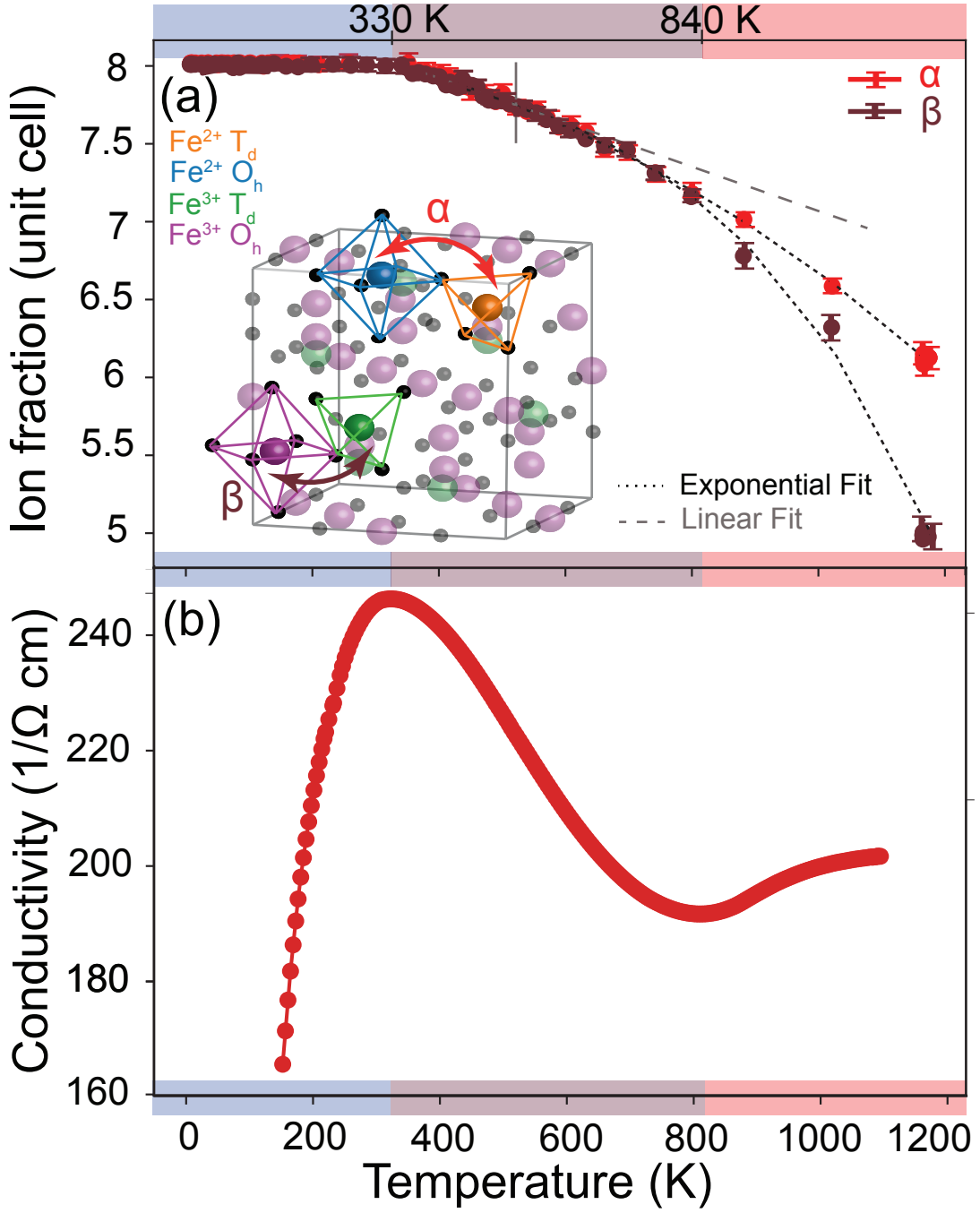

FIG. 3. (a) Temperature evolution of the redistribution parameters α (red) and β (brown) in Fe_3O_4. Linear and exponential fits are plotted in dashed gray and black dashed lines. A cartoon of the ion transfer in a unit cell of Fe_3O_4 is shown in the inset. (b) Temperature dependence of the electrical conductivity of Fe_3O_4. The colour code on the x-axis of the figure illustrates the regimes described in the text.

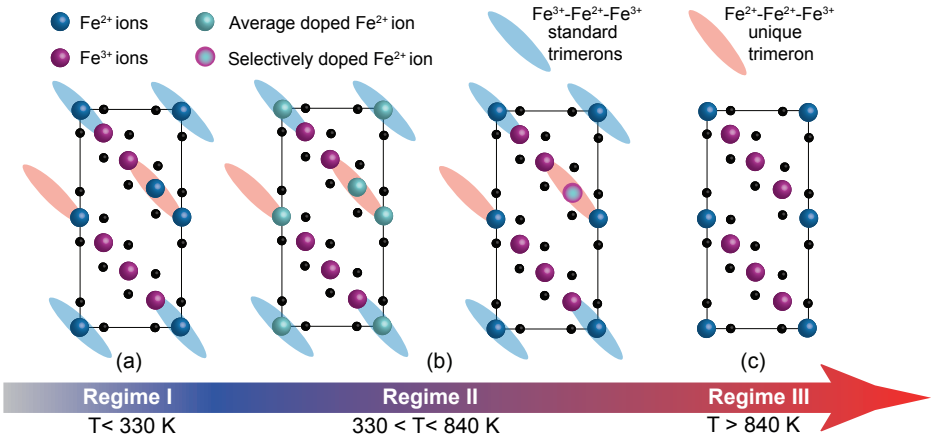

FIG. 4. Proposed possible model for the effect of temperature on Fe_3O_4. The Cc supercell is shown with the (100) surface of cubic magnetite showing trimerons (shadowed) in the surface layer. Only the B-sites are shown where the Fe^{2+}-like and Fe^{3+}-like ions are plotted in blue and purple respectively. Oxygen is shown in black. The B42 like-site is shown encompassed with a red trimeron. (a) In regime I, local correlations in Fe_3O_4 resemble that of the low temperature phase. (b) Self-doping occurs in regime II where initially the entire unit cell mitigates the hole and depicted in light blue. At the self-doping $\delta = 0.023$, the hole localizes on a single trimeron. (d) Increasing the self-doping level beyond a critical level where the Fe^{2+} B42 like-site fully oxidizes to Fe^{3+} leads to the collapse of all local correlations. We emphasize that the current illustration represents a proposed snapshot in time of structural fluctuations.

In this work we propose an elegant analogy between the temperature-driven self-doping at the B-sublattice far above the Verwey temperature and the chemical doping effect observed at low temperature (Fig. 4). We propose that the changeover from the linear temperature dependence of the charge ordering is triggered by a critical hole self-doping level of 0.023 (reached at T=500 K as seen in Fig. S10) similar to the effect of doping on the Verwey transition [43]. Essentially before this level of doping, the short-range trimeron are not significantly perturbed and we suspect that the partial hole doped into the B sublattice is mitigated by the entire dynamical network. As the self-doping level increases above ~ 0.023, Fe_3O_4 transitions to a selective self-doping on one precise trimeron. We emphasize that at these temperatures trimerons are not static, however, per snapshot, the self-doped hole resides on one trimeron selectively as evidenced by the local Jahn-Teller distortion observed by XAS. The selective self-doping progresses until the Fe^{2+} cation is fully oxidised to Fe^{3+}

(i.e. B-site Fe^{3+}:Fe^{2+}= 9 : 7 as seen in Fig. 3). This considerable perturbation is of a critical consequence: the trimerons completely breakdown. The signature of this is imprinted on the collapse of magnetism (Fig. S9 [44]) and the changeover of the electrical conductivity (Fig.3(b)).

In summary, this work demonstrates that a charge reordering occurs in Fe_3O_4 from 330 K leading to a contineous and reversible hole self-doping effect at the B-sublattice. Despite its simplicity, our model captures the prominent features of our experimental data and suggests that α and β are adequate descriptors for correlations in Fe_3O_4. Temperature driven self-doping provides a unique adjustable experimental handle intimately connected to chemical doping. Beyond these results, we envision using the combination of K pre-edge HERFD-XAS and theoretical calculations to solve open questions in palaeomagnetism where understanding correlations in iron minerals under high pressure and temperatures is essential.

ACKNOWLEDGEMENTS

We are grateful to the help of the scientists at beamline ID 26, the sample environment and the safety group of the European Synchrotron Radiation Facility. We are also thankful to M. van der Linden and P. Zimmermann for their assistance during the beamtime. A. Juhin, D. Cabaret, Ph. Sainctavit and F. Meirer are thanked for the fruitful discussions. This work was financed by the ERC advanced Grant XRAYonACTIVE No. 340279. H.E. acknowledges the finance of NWO Rubicon Fellowship (project number 019.201EN.010). W.T. and M.A.G. acknowledge financing provided by the Polish National Agency for Academic Exchange under "Polish Returns 2019" Programme: PPN/PPO/2019/1/00014/U/0001, and subsidy of the Ministry of Science and Higher Education of Poland.

* H.M.E.A.Elnaggar@uu.nl

† F.M.F.degroot@uu.nl

[1] T. P. Almeida, T. Kasama, A. R. Muxworthy, W. Williams, L. Nagy, T. W. Hansen, P. D. Brown, and R. E. Dunin-Borkowski, Nat. Commun. **5**, 5154 (2014).

[2] I. A. M. Ahmeda and B. A. Maher, Proc. Natl. Acad. Sci. **115**, 1736 (2018).

[3] J. A. Tarduno, R. D. Cottrell, R. K. Bono, H. Oda, W. J. Davis, M. Fayek, O. v. '. Erve, F. Nimmo, W. Huang, E. R. Thern, S. Fearn, G. Mitra, A. V. Smirnov, and E. G. Blackman, Proc. Natl. Acad. Sci. **117**, 2309 (2020).

[4] S. Veintemillas-Verdaguer, M. Marciello, M. P. Morales, C. J. Serna Pereda, and M. Andrés-Vergés, Prog. Cryst. Growth Charact. Mater. **60**, 80 (2014).

[5] B. Duong, H. Khurshid, P. Gangopadhyay, J. Devkota, K. Stojak, H. Srikanth, L. Tetard, R. A. Norwood, N. Peyghambarian, M. Phan, and J. Thomas, Small **10**, 2840 (2014).

[6] N. Pontius, T. Kachel, C. Schüßler-Langeheine, W. F. Schlotter, M. Beye, F. Sorgenfrei, C. F. Chang, A. Föhlisch, W. Wurth, P. Metcalf, I. Leonov, A. Yaresko, N. Stojanovic, M. Berglund, N. Guerassimova, S. Düsterer, H. Redlin, and H. A. Dürr, Appl. Phys. Lett. **98**, 182504 (2011).

[7] S. de Jong, R. Kukreja, C. Trabant, N. Pontius, C. F. Chang, T. Kachel, M. Beye, F. Sorgenfrei, C. H. Back, B. Bräuer, W. F. Schlotter, J. J. Turner, O. Krupin, M. Doehler, D. Zhu, M. A. Hossain, A. O. Scherz, D. Fausti, F. Novelli, M. Esposito, W. S. Lee, Y. D. Chuang, D. H. Lu, R. G. Moore, M. Yi, M. Trigo, P. Kirchmann, L. Pathey, M. S. Golden, M. Buchholz, P. Metcalf, F. Parmigiani, W. Wurth, A. Föhlisch, C. Schüßler-Langeheine, and H. A. Dürr, Nat. Mater **12**, 882 (2013).

[8] D. Dunlop and O. Özdemir, *Rock Magnetism* (Cambridge Univ. Press., 1997).

[9] E. J. W. Verwey, Nature **144**, 327 (1939).

[10] W. H. Bragg, Nature **95**, 561 (1915).

[11] M. S. Senn, J. P. Wright, and J. P. Attfield, Nature **481**, 173 (2012).

[12] G. Perversi, E. Pachoud, J. Cumby, J. M. Hudspeth, J. P. Wright, S. A. J. Kimber, and J. Paul Attfield, Nat. Commun. **10**, 2857 (2019).

[13] A. Bosak, D. Chernyshov, M. Hoesch, P. Piekarz, M. Le Tacon, M. Krisch, A. Kozłowski, A. M. Oleś, and K. Parlinski, Phys. Rev. X **4**, 011040 (2014).

[14] H. Y. Huang, Z. Y. Chen, R. P. Wang, F. M. F. de Groot, W. B. Wu, J. Okamoto, A. Chainani, A. Singh, Z. Y. Li, J. S. Zhou, H. T. Jeng, G. Y. Guo, J.-G. Park, L. H. Tjeng, C. T. Chen, and D. J. Huang, Nat. Commun. **8**, 15929 (2017).

[15] H. Elnaggar, R. Wang, S. Lafuerza, E. Paris, A. C. Komarek, H. Guo, Y. Tseng, D. McNally, F. Frati, M. W. Haverkort, M. Sikora, T. Schmitt, and F. M. F. de Groot, Phys. Rev. B **101**, 085107 (2020).

[16] R. J. McQueeney, M. Yethiraj, S. Chang, W. Montfrooij, T. G. Perring, J. M. Honig, and P. Metcalf, Phys. Rev. Lett. **99**, 246401 (2007).

[17] C. Gauthier, V. A. Solé, R. Signorato, J. Goulon, and E. Moguiline, Journal of Synchrotron Radiation **6**, 164 (1999).

[18] P. Glatzel, T.-C. Weng, K. Kvashnina, J. Swarbrick, M. Sikora, E. Gallo, N. Smolentsev, and R. A. Mori, Journal of Electron Spectroscopy and Related Phenomena **188**, 17 (2013).

[19] K. Hämäläinen, D. P. Siddons, J. B. Hastings, and L. M. Berman, Phys. Rev. Lett. **67**, 2850 (1991).

[20] M. Wilke, F. Farges, A. Juhin, P.-E. Petit, J. Brown, Gordon E., and F. Martin, Am. Mineral. **86**, 714 (2001).

[21] M. Wilke, O. Hahn, A. B. Woodland, and K. Rickers, J. Anal. At. Spectrom. **24**, 1364 (2009).

[22] H. Elnaggar, P. Sainctavit, A. Juhin, S. Lafuerza, F. Wilhelm, A. Rogalev, M.-A. Arrio, C. Brouder, M. van der Linden, Z. Kakol, M. Sikora, M. W. Haverkort, P. Glatzel, and F. M. F. de Groot, Phys. Rev. Lett. **123**, 207201 (2019).

[23] T. E. Westre, P. Kennepohl, J. G. DeWitt, B. Hedman, K. O. Hodgson, and E. I. Solomon, J. Am. Chem. Soc. **119**, 6297 (1997).

[24] M.-A. Arrio, S. Rossano, C. Brouder, L. Galoisy, and G. Calas, Europhys. Lett. **51**, 454 (2000).

[25] V. Vercamer, M. O. J. Y. Hunault, G. Lelong, M. W. Haverkort, G. Calas, Y. Arai, H. Hijiya, L. Paulatto, C. Brouder, M.-A. Arrio, and A. Juhin, Phys. Rev. B **94**, 245115 (2016).

[26] M. W. Haverkort, M. Zwierzycki, and O. K. Andersen, Phys. Rev. B **85**, 165113 (2012).

[27] M. Retegan, "Crispy: v0.7.3," (2019).

[28] C. Wu and T. Mason, J. Am. Ceram. Soc. **64**, 520 (1981).

[29] D. Levy, R. Giustetto, and A. Hoser, Phys. Chem. Minerals **39**, 1432 (2012).

[30] L. Häggström, H. Annersten, T. Ericsson, R. Wäppling, W. Karner, and S. Bjarman, Hyperfine Interactions **5**, 1572 (1977).

[31] S. Wissmann, V. Wurmb, F. J. Litterst, R. Dieckmann, and K. D. Becker, J. Phys. Chem. Solids **59**, 321 (1998).

[32] R. Dieckmann and H. Schmalzried, Berichte der Bunsengesellschaft für physikalische Chemie **81**, 344 (1977).

[33] F. Pedregosa, G. Varoquaux, A. Gramfort, V. Michel, B. Thirion, O. Grisel, M. Blondel, P. Prettenhofer, R. Weiss, V. Dubourg, J. Vanderplas, A. Passos, D. Cournapeau, M. Brucher, M. Perrot, and E. Duchesnay, Journal of Machine Learning Research **12**, 2825 (2011).

[34] R. Dieckmann and H. Schmalzried, Berichte der Bunsengesellschaft für physikalische Chemie **81**, 414 (1977).

[35] R. Dieckmann, T. O. Mason, J. D. Hodge, and H. Schmalzried, Berichte der Bunsengesellschaft für physikalische Chemie **82**, 778 (1978).

[36] R. Dieckmann, Berichte der Bunsengesellschaft für physikalische Chemie **86**, 112 (1982).

[37] R. Dieckmann, C. A. Witt, and T. O. Mason, Berichte der Bunsengesellschaft für physikalische Chemie **87**, 495 (1983).

[38] R. Dieckmann and H. Schmalzried, Berichte der Bunsengesellschaft für physikalische Chemie **90**, 564 (1986).

[39] Brabers, V. A. M. and Klerk, J., J. Phys. Colloques **38**, C1 (1977).

[40] H. Okudera, K. Kihara, and T. Matsumoto, Acta Crystallographica Section B **52**, 450 (1996).

[41] J. M. Honig, Journal of Alloys and Compounds **229**, 24 (1995).

[42] V. A. M. Brabers, F. Walz, and H. Kronmüller, Phys. Rev. B **58**, 14163 (1998).

[43] E. Pachoud, J. Cumby, G. Perversi, J. P. Wright, and J. P. Attfield, Nat. Commun. **11**, 1671 (2020).

[44] I. Biało, A. Kozłowski, M. Wack, A. Włodek, . Gondek, Z. Kąkol, R. Hochleitner, A. Żywczak, V. Chlan, and S. A. Gilder, Geophysical Journal International **219**, 148 (2019).